Published in final edited form as:
Biomaterials. 2008 May ; 29(15): 2336–2347.

Microvascular Maturity Elicited in Tissue Treated with Cytokine-loaded Hyaluronan-based Hydrogels

Luke W. Hosack[1], **Matthew A. Firpo**[2], **J. Anna Scott**[3], **Glenn D. Prestwich**[4], and **Robert A. Peattie**[5]

1*Department of Chemical Engineering, Oregon State University, Corvallis, OR 97331*

2*Department of Surgery, University of Utah School of Medicine, Salt Lake City, UT 84132*

3*Glycosan BioSystems, Inc., 675 Arapeen Way, Suite 302, Salt Lake City, UT 84108*

4*Center for Therapeutic Biomaterials, Department of Medicinal Chemistry, University of Utah, Salt Lake City, UT 84108*

5*Department of Biomedical Engineering, Tufts University, Medford, MA 02155*

Abstract

Hydrogels composed of crosslinked, chemically modified hyaluronic acid (HA), gelatin (Gtn) and heparin (Hp) were preloaded with vascular endothelial growth factor (VEGF), angiopoietin-1 (Ang-1), keratinocyte growth factor (KGF) or platelet derived growth factor (PDGF) either individually or in combination with VEGF and implanted into the Balb/c mouse ear pinna. At 7 and 14 days post-surgery, elicited vascular maturity levels were quantified using immunohistochemical (IHC) staining techniques and reported as a vascular maturity index (VMI). At both time points, it was discovered that the dual cytokine combinations elicited greater maturity levels than either cytokine administered individually. For example, VEGF and KGF-containing HA:Hp implants at day 7 yielded VMI values of −0.1375 and −0.092, respectively, whereas their combination resulted in a VMI of 0.176 ($p < 0.007$). At day 7, only one of the seven HA:Hp experimental cases yielded a positive VMI (VEGF+KGF), whereas four of the seven HA:Hp cases yielded positive VMI values at day 14, indicating a sustained maturity response. The same general trends were found to exist in tissue treated with HA:Hp:Gtn experimental implants. Differences in elicited maturity also existed between tissue treated with HA:Hp and HA-containing hydrogels (VMI = 0.176 for HA:Hp-VEGF +KGF *vs.* −0.064 for HA-VEGF+KGF, $p < 0.012$), and these differences are thought to result from differences in characteristic cytokine release rates. This result also suggests that the presentation of multiple GFs on immobilized Hp may actively contribute to cytokine related signal transduction; a characteristic that may be exploited in the future to improve the efficacy of cytokine-loaded implants towards tissue regeneration therapeutic strategies.

Keywords

Angiogenesis; Animal Model; Immunohistochemistry; Cytokine; Glycosaminoglycan; Controlled Drug Release; Gelatin

Correspondence: Luke W. Hosack, 2781 NW Overlook Dr. #415, Hillsboro, OR 97124, hosackl@onid.orst.edu, (541) 231-6844 (phone).

1. INTRODUCTION

A simple and effective technology for sustaining *in vivo* tissue regeneration would offer the possibility of new approaches to treatment of many types of diseases, such as pathologies of bone, blood vessels, heart and skeletal muscle, liver and many other tissues and organs [1]. At present, however, implanted cell and tissue growth is limited by inadequate vascularization and the resulting insufficient respiratory gas transport [2]. Delivery of appropriate factors along with the implanted cells, to induce a supporting angiogenic response, has the potential to overcome this difficulty. It has been shown by many investigators that angiogenesis can be achieved through therapeutic cytokine delivery [3–5]. However, the long term viability and functionality of capillary networks elicited by exogenous cytokines has not been demonstrated [6].

The primary impediments to controlling localized microvessel growth arise from the intricacy of angiogenesis and the complexity of the signals by which vessel growth is regulated. Natural capillary development is a central aspect of many physiologic and pathologic functions, including tissue and organ growth, wound healing, female reproductive function, and tumor formation [7]. Formation of new microvessels from existing vessel beds is typically initiated within oxygen depleted tissue [8]. Vascular endothelial growth factor (VEGF) originating from hypoxic sites imparts a strong mitogenic effect on endothelial cells of the neighboring microvasculature, mediated through a receptor tyrosine kinase (RTK) signal cascade [9]. VEGF has also been shown to upregulate the endothelial cell-associated production of matrix metalloproteinase enzymes (MMPs) [7]. These MMPs degrade the surrounding basement membrane and extracellular matrix (ECM), allowing proliferating endothelial cells to migrate towards the site of hypoxia and form new capillary sprouts. These sprouts eventually anastomose to form new perfusable microvessel loops [10].

As nascent loops begin to take shape, microvascular endothelial cells also begin producing platelet derived growth factor (PDGF). PDGF binds to specific smooth muscle pericyte receptors, stimulating pericyte migration and proliferation [11]. New pericytes stabilize the nascent microvasculature by orchestrating the formation of an extensive basement membrane [12]. Pericytes are also responsible for the production of Angiopoetin-1 (Ang-1), a ligand for the Tie-2 RTK receptor found on endothelial cells that promotes endothelial cell survival and continued pericyte association [13]. New vessels reach maturity when contiguous vessels connect, a new basement membrane is formed and smooth muscle pericytes associate with this basement membrane [12]. Extensive research suggests that nascent microvessels are complete and stable once fully ensheathed by pericytes [14–16].

One of the primary hypotheses underlying our studies is that implantation of devices capable of releasing appropriate sequences of growth factors (GFs) *in situ* with desired timing can promote angiogenesis and thereby elicit enduring, mature blood vessel networks. Hydrogels fabricated from chemically modified hyaluronic acid (HA) can serve as ideal biocompatible substrates for release of cytokine combinations *in vivo* [17–21]. HA consists of repeating disaccharide units (β-1,4-D-glucuronic acid—β-1,3-N-acetyl-D-glucosamine) with an overall molecular weight between 100 kDa and 5000 kDa. The macroporous nature of hydrogels based on HA provides a means for storage and delivery of cytokines, while the glycosaminoglycan structure mimics native ECM. Moreover, the small oligosaccharides released as HA breaks down are strong angiogenic promoters [22]. Consequently, HA-based films actively participate in the tissue response, rather than merely serving as passive conveyance mechanisms. In addition to these properties, it has been shown that addition of small amounts of chemically modified heparin (Hp) to HA-based gels results in sustained growth factor release [20,23,24]. N- and O-sulfated residues of heparin interact with lysine and arginine residues of GFs [20, 25,26]. Presumably, heparin in the ECM plays a storage role for GFs, slowing their release

while retaining their bioactivity. Heparin binding is also thought to stabilize GFs against thermal denaturation as well as degradation by ECM proteinases [25].

In this study, it was hypothesized that *in vivo* implantation of crosslinked, chemically-modified HA and HA+Gelatin (Gtn) hydrogels pre-loaded with two cytokines and containing small quantities of immobilized and co-crosslinked Hp (0.3% w/w) would elicit the growth of more stable and mature microvessel beds than in the absence of Hp. The gels were loaded with one factor selected to initiate an angiogenic response, VEGF, and a second to promote neovessel maturation, either PDGF-AA, keratinocyte growth factor (KGF) or Ang-1. Each of these has been linked to pericyte recruitment, proliferation and/or endothelial cell association [11,27, 28]. The hypothesis was tested by quantifying the levels of tissue microvessel maturity at fixed times post-implantation, using established immunohistochemical (IHC) staining techniques based on the degree of circumferential pericyte ensheathement [14–16].

2. MATERIALS AND METHODS

2.1 Materials

Fermentation-derived hyaluronic acid (sodium salt, M_W = 750 kDa) (HA) was from Novozymes Biopolymers (Copenhagen, Denmark). Heparin (sodium salt from porcine mucosa, unfractionated, M_W = 15 kDa) (Hp) and gelatin (bovine skin, type B, gel strength approximately 225 Bloom) (Gtn) were purchased from Sigma Chemical Co. (St. Louis, MO). Polyethylene glycol (M_W = 3400 Da) (PEG), 1-ethyl-3-[3-(dimethylamino)propyl] carbodiimide (EDCI), hydrazine hydrate and 3,3'-dithiobis(propanoic acid) (DTP) were acquired from Aldrich Chemical Co. (Milwaukee, WI). Dithiothreitol (DTT) was from Diagnostic Chemicals Limited (Oxford, CT). Vascular endothelial growth factor (human recombinant, 165 amino acid, M_W = 38.2 kDa) (VEGF), keratinocyte growth factor (human recombinant, 163 amino acid, M_W = 18.9 kDa) (KGF) and platelet derived growth factor (human recombinant, 250 amino acid, M_W = 28.5 kDa) (PDGF) were purchased from Peprotech, Inc. (Rocky Hill, NJ). Angiopoietin-1 (human recombinant, 476 amino acid, M_W = 66 kDa) (Ang-1) was purchased from Sigma Chemicals Co. (St. Louis, MO). Smooth muscle α-actin (α-SMA) rabbit monoclonal antibody was purchased from Epitomics (Burlingame, CA). Rabbit polyclonal antibody to von Willebrand factor (vWF) was provided by Oregon State University Veterinary Medicine Diagnostic Laboratory, and purchased from Dako (Glostrup, Denmark). Male Balb/c AnNCr mice age approximately 5–6 weeks were purchased from NCI (Frederick, MD).

2.2 Chemical syntheses

Thiol-modified HA, gelatin and heparin were synthesized as previously reported [29]. Briefly, these hydrogel components were modified with 3,3'-dithiolbis(propanoic hydrazide) in an EDCI-mediated condensation reaction, followed by DTT reduction and dialysis. The structures were confirmed and tested for purity using ^{1}H-NMR and GPC. The degree of thiol substitution for each hydrogel component was determined by a modified DTNB method [30], and was 42%, 56% and 37% of available carboxylate groups for HA-DTPH, Hp-DTPH and Gtn-DTPH, respectively. Poly(ethylene glycol)-diacrylate (PEGDA) was synthesized from PEG by previously described procedures [31].

2.3 Hydrogel film preparation

Two different sets of HA-based hydrogels were prepared, either including or omitting modified gelatin as a matrix component. All gels incorporated the same quantity of modified heparin, 0.3% Hp-DTPH w/w relative to HA-DTPH, or in the gelatin-containing gels, 0.3% Hp-DTPH w/w relative to HA-DTPH + Gtn-DTPH. For gels lacking gelatin, HA-DTPH and Hp-DTPH were dissolved together in PBS in an amount to achieve 1.25% w/v (g/mL) HA-DTPH.

Separately, PEGDA was dissolved in PBS to achieve 4.4% w/v (g/mL) PEGDA. Both solutions were brought to pH 7.4. Prior to crosslinking, the appropriate cytokine or cytokine combination was added to the HA:Hp solution in a quantity to achieve 100 ng of each cytokine per implant. The PEGDA solution was then added to the HA:Hp:cytokine solution in a 1:4 volume ratio (PEGDA:HA), giving a 1:2 ratio of acrylate to thiol functionalities. The resulting solution was maintained under gentle agitation on an orbital rotator for 24 hours, then dehydrated at 37°C to form a durable, flexible 1-mm thick film. At the time of surgery, the film was retrieved from 4°C storage and 4-mm diameter disks were cut for implantation.

An identical procedure was followed for synthesizing gelatin-containing gels, save that half of the HA-DTPH was replaced with Gtn-DTPH (Figure 1).

2.4 Surgical and experimental procedure

All procedures were carried out with the full approval of the Oregon State University Institutional Animal Care and Use Committee. Male Balb/c AnNCr mice aged 5–6 weeks were anesthetized with 2.5% isoflurane by volume using an inhalation anesthesia system (Summit Medical Equipment Inc., Bend, OR). Once a deep general anesthetic plane had been reached, a shallow 4–5mm incision was made through the superficial skin on the posterior pinna of the right ear. A blunt probe was inserted through the incision, and a 5-mm pocket was created under the skin. If the animal was to receive an implant, the 4-mm cytokine-loaded HA- or HA:Gtn film was placed inside the pocket and the incision was closed without sutures. Mice recovered from this brief procedure without incident within minutes, and the incision healed in 5–7 days.

On days 7 or 14 days post-implantation, the mice were anesthetized by overdose with isoflurane (5%) and immediately sacrificed by cervical dislocation. The surgical and contralateral ears were retrieved and fixed in formalin overnight, then embedded in paraffin. Tissue blocks were thin-sectioned in planes parallel to the plane of the pinna and double stained by immunohistochemical techniques, using antibodies against α-SMA and vWF proteins [see ref 32 for details]. Briefly, primary α-SMA monoclonal antibody diluted 1:100 was applied followed by HRP-conjugated secondary antibody and the chromagen DAB for visualization. High temperature antigen retrieval for vWF was then performed. A primary polyclonal vWF antibody diluted 1:400 was applied, followed by HRP-conjugated secondary antibody and Nova Red for visualization.

Identification marks on each slide were covered so that the observer was blind to the treatment group. The slide was then viewed under light microscopy at 100× magnification to determine consistency of staining and overall distribution of stained microvessels, including the extent of intense localized neovascularization. Five 250 μm^2 fields were chosen for quantification, with a representative number of the five fields devoted to these highly dense and often primitive microvascular networks. The remaining fields were devoted to areas of relatively mature microvasculature.

Microvessels in each field were counted directly at 400× magnification. The maturity of each microvessel was evaluated according to the visible integrity of its endothelial border, indicated by vWF staining (red), as well as by the degree of circumferential pericyte ensheathement, shown by α-SMA (brown). Vessels were assigned to one of three bins, with each bin representing a population of microvessels displaying a distinct level of maturity (Figure 2).

2.5 Data Analysis

A total of three animals received implants for each treatment case, at each time point ($n = 3$). To account for both the number of microvessels present prior to surgery and nonspecific new

microvessel growth secondary to surgical probing, so that the influences of the film and/or growth factor(s) on new microvessel formation would be identifiable, a dimensionless neovascularization index (NI) was defined as

$$\mathrm{NI} = \frac{\overline{\left(\sum_{i=1}^{3} n_i\right)}_{\text{Surgical ear}} - \overline{\left(\sum_{i=1}^{3} n_i\right)}_{\text{Sham ear}}}{\overline{\left(\sum_{i=1}^{3} n_i\right)}_{\text{Contralateral ear}}} \quad (1)$$

where i represents bin number and n_i represents the number of microvessels in the i^{th} bin. In particular, $\overline{\left(\sum_{i=1}^{3} n_i\right)}_{\text{Surgical ear}}$ represents the total microvessel count in all bins in the surgical ear, averaged over all animals in a given treatment group, and the other sums represent the total count in the sham control that underwent pocket formation but received no implant and the contralateral ear, respectively. Accordingly, *NI* represents the number of additional vessels present post-implant in a treatment group, minus the additional number due to the surgical procedure alone, normalized by the contralateral count [17–20].

To account for the microvascular maturity levels present before surgery as well as those induced by the surgical procedure, so that the effect of the film and/or cytokine(s) could be identified, a corresponding dimensionless vascular maturity index (VMI) was defined as

$$\mathrm{VMI} = \frac{\overline{\left(\frac{\sum_{i=1}^{3} n_i i}{\sum_{i=1}^{3} n_i}\right)}_{\text{Surgical ear}} - \overline{\left(\frac{\sum_{i=1}^{3} n_i i}{\sum_{i=1}^{3} n_i}\right)}_{\text{Sham ear}}}{\overline{\left(\frac{\sum_{i=1}^{3} n_i i}{\sum_{i=1}^{3} n_i}\right)}_{\text{Contralateral ear}}}. \quad (2)$$

Specifically, the ratio $\overline{\left(\frac{\sum_{i=1}^{3} n_i i}{\sum_{i=1}^{3} n_i}\right)}_{\text{Surgical ear}}$ represents the microvessel maturity level found in the treated ear, calculated as the weighted sum of microvessel counts over all bins (1–3) divided by the total microvessel count, averaged over the animals in a treatment group. Similarly, the other sums represent the maturity level in the sham control and contralateral ears. Thus defined, *VMI* represents the total microvessel maturity response elicited in a treatment group, minus the maturity of vessels healing from surgical manipulation of the ear, normalized to the static microvessel maturity levels of the contralateral ear.

NI and *VMI* values were determined at both 7 and 14 days post film implantation. All data sets were compared using two-tailed, unpaired *t*-tests; values of $p \leq 0.05$ were considered significant. Data are presented as mean ± standard deviation.

3. RESULTS

New *in vivo* microvessel development and maturation was assessed in an ear pinna model for a series of experimental conditions including (i) an HA:Hp film preloaded with VEGF; (ii) an HA:Hp film preloaded with Ang-1; (iii) an HA:Hp film preloaded with KGF; (iv) an HA:Hp film preloaded with PDGF-AA; and (v–vii) HA:Hp films all preloaded with VEGF along with KGF, Ang-1 or PDGF-AA. In addition, the same seven experimental cases were studied using films containing equal parts HA and Gtn (HA:Hp:Gtn) (viii–xiv). Control cases included a sham surgery in which a pocket was formed but no implant was delivered (xv), HA (xvi) and HA:Hp (xvii) films without preloaded cytokines, and HA films preloaded with both VEGF and KGF (xviii), or VEGF and Ang-1 (xix). These controls allow for direct evaluation of the neovascular and maturity effects attributable to the individual film components, as well as to interaction between preloaded cytokines and immobilized and co-crosslinked heparin.

Representative photographic images of microvasculature at 7 days post-surgery show significant differences that characterized the tissue response to each treatment condition (Figure 3). Contralateral ear sections had a similar appearance for all animals (Figure 3a). No evidence of any systemic response to the implant was observable at either experimental time point for any of the treatment cases. Chondrocytes were widely distributed in this tissue, along with numerous hair follicles and sebaceous and other glands. Contralateral ears exhibited relatively low vessel densities, however, the existing vasculature was very well developed.

Ears implanted with VEGF pre-loaded HA:Hp disks continued to show the chondrocytes, hair follicles and glands typical of ear pinnas. However, there were large numbers of primitive, high density, incomplete microvessel networks (Figure 3b). These vessels lacked a complete endothelial border, which created the appearance of hyperfused microvascular lumina. In general, tissue treated with VEGF-loaded HA:Hp films exhibited high microvessel density with poorly defined borders and little to no pericyte ensheathement.

By far the most mature vasculature elicited in the HA:Hp experimental cases at 7 days post implantation was found in ears treated with VEGF+KGF (Figure 3c). These microvessels exhibited clearly defined endothelial borders with extensive pericyte ensheathement. The surrounding tissue showed a normal distribution of chondrocytes, hair follicles and glands. Both the tissue and the elicited microvasculature appeared mature and fully developed for this treatment.

Microvascular density was analyzed quantitatively through the neovascularization index (Figure 4 and Figure 5). For both NI and VMI, positive values indicate a tissue response greater than that of sham control ears, while negative values indicate a lesser response than sham. At 7 days post implantation (Figure 4a), HA:Hp-VEGF treated tissue exhibited the highest levels of neovascular density (NI = 3.06), followed by the HA:Hp-KGF and HA:Hp-Ang-1 treatment cases (NI = 2.44 and 1.81, respectively). There was a significant difference in the tissue response to heparinized VEGF+KGF treatment compared to the non-heparinized case (NI = −0.174 and 1.57, respectively; $p < 0.05$), but that difference was not maintained for other dual growth factor combinations.

On day 14 (Figure 4b), although the HA:Hp-VEGF case again yielded the highest neovascular response (NI = 0.90), it was the only case to show significantly more vascularization than the sham control ($p < 0.04$). Moreover, the response to this treatment was substantially less than at day 7. In fact, a decrease in NI from 7 to 14 days post implantation was evident in nearly all control and experimental tissues, including those treated with HA:Hp:Gtn films (Figure 5).

The maturity of elicited microvessel beds was assessed quantitatively through VMI values (Figure 6). At 7 days post film-implantation (Figure 6a), the only treatment case exhibiting

greater maturity than sham surgery was HA:Hp-VEGF+KGF (VMI = 0.176). Accordingly, treatment with VEGF+KGF produced a microvascular maturity response statistically significantly superior to all other treatments ($p < 0.03$). In general, higher levels of vascular maturity were achieved in tissue treated with a dual cytokine combination when compared to the response elicited by either cytokine individually. For example, the HA:Hp-VEGF+KGF treated tissue was significantly superior to both HA:Hp-VEGF (VMI = −0.138; $p < 0.004$) and HA:Hp-KGF (VMI = −0.092; $p < 0.008$). The heparinized VEGF+KGF dual cytokine case also yielded significantly higher VMI values than its corresponding non-heparinized control (VMI = −0.064; $p < 0.01$).

Microvasculature was much more mature for all experimental and control cases at 14 days than at 7 days post-surgery, as reflected by striking increases in VMI values over the second week (Figure 6b). HA:Hp films containing the VEGF+KGF and VEGF+PDGF dual cytokine combinations elicited the most mature vasculature at day 14 (VMI = 0.103 and 0.159, respectively). Many of the trends evident at day 7 continued to exist at day 14. Specifically, the dual cytokine combinations continued to elicit microvasculature that was more mature than either cytokine delivered individually. Figure 6b also shows that the heparinized VEGF+Ang-1 experimental dual cytokine treatment yielded significantly lower VMI values compared to the non-heparinized control (VMI = −0.41 and 0.126, respectively; $p < 0.05$).

Figure 7 presents VMI values from cytokine-loaded HA:Hp:Gtn treated tissue at both 7 days (left) and 14 days (right) post film-implantation. The most mature vasculature at 7 days was found in the VEGF+PDGF dual cytokine treated tissue (VMI ≈ 0). The 14 day Gtn treatments yielded results that were consistent with those seen at 7 days post-implantation, in that VEGF and VEGF+PDGF again elicited maturity responses that were among the least and most favorable, respectively (VMI = −0.090 and 0.128). As with non-gelatinized cases, VMI increased from day 7 to day 14 for all treatments. In general, the Gtn-containing experimental films at both time points yielded microvascular maturity responses that were statistically indistinguishable from the corresponding HA:Hp gels.

4. DISCUSSION

The capacity of HA hydrogel film implants to induce the development of new capillary networks *in vivo* by localized delivery of pre-loaded cytokines has been well demonstrated in previous experiments [17–20]. Vessel development is amplified by the ability of HA and growth factors to potentiate each other's activity, which leads to a strong angiogenic response even when the growth factors are delivered in very low ng doses. Furthermore, heparin regulation of multiple growth factor delivery produces neovessel beds without inappropriate permeability or extravasation of red cells at two weeks post-implantation [17,20].

The IHC approach used here to characterize elicited neovascular density gave results that were consistent with previous experiments using hematoxylin and eosin staining in many important ways. For example, Riley *et al.* found NI values to decrease from 7 to 14 days post implantation [17], a trend also realized in the current study. In addition, at 14 days post heparinized film implantation, Riley *et al.* found NI to increase in the order HA:Hp, HA:Hp-Ang-1, HA:Hp-VEGF and HA:Hp-VEGF+Ang-1. A very similar pattern was also realized in the present experiment (Figure 4b). Such a correspondence is not as automatic as might be thought, since H&E staining visualizes microvessels indirectly, primarily by highlighting contiguous red blood cell chains. However, treated tissue can exhibit considerable RBC extravasation, which leads to the possibility of overestimating neovascular density. In contrast, IHC staining for the constitutive endothelial cell marker vWF marks vessel walls directly. As a result, it is not surprising that previous studies [17] reported generally higher NI values than were found here. More importantly, however, many similar trends were nevertheless evident in the data.

One of the most striking results of this study is that at day 7, all the control cases and all but one of the experimental cases showed maturity less than sham ears (Figure 6a). In contrast, by day 14 all the control cases and four of the seven experimental cases showed greater vessel maturity than sham ears (Figure 6b). This pattern would be expected for tissue recovering from the surgical procedure and responding successfully to many of the treatments.

Inclusion of heparin in the film had a cytokine-dependent influence on microvessel maturity levels, improving maturation in some cases but inhibiting maturation in others. For example, a significant improvement was found for the maturity of vessel beds elicited by co-release of the dual growth factors VEGF+KGF from heparin-containing films compared to their release from non-heparinized films (VMI = 0.176 and −0.064 respectively at 7 days post-implantation, $p < 0.01$, Figure 6a). Thus, the inclusion of heparin in the gels had a significant positive influence on vessel maturation for this particular treatment. This effect has been demonstrated in other related studies [33]. Conversely, release of the growth factor combination VEGF +Ang-1 from heparin-containing gels produced vessels with significantly less maturity than their release from non-heparinized gels (VMI = −0.41 and 0.126 respectively at day 14, $p < 0.05$, Figure 6b), suggesting that the inclusion of heparin had a negative influence.

The maturity levels of new microvessels are produced by the simultaneous effects of both physical and biologic processes. Physically, at early times following implantation, diffusional transport of growth factors out of the gel can be expected to deplete the gel perimeter and establish growth factor concentration gradients around and within the implant (Figure 8). Such VEGF chemotactic gradients have been found to guide proliferating microvascular tip cells *in vivo* [34]. At the same time, endogenous tissue-resident hyaluronidase begins to break down the gel, creating pathways for microvascular invasion. Furthermore, migratory tip cells are known to secrete PDGF. Elicited PDGF can be expected to promote the concomitant migration of pericytes into the gel along with the endothelial cells [35]. Accordingly, it is not unreasonable to anticipate the initiation of microvascular growth around and into the gels.

Endothelial cell proliferation (neoangiogenesis) and pericyte division and vessel coverage (maturation) are separate stages of the angiogenic response. Since they are driven by separate cytokine signals, vessel maturation depends on exposure to the secondary growth factor. However, the amounts of early and late stage cytokine available at the hydrogel perimeter are dictated by the characteristic rates at which each is released from the hydrogel matrix. *In vitro* release measurements performed as part of a different study indicate that heparin-containing gels release different GFs at specific rates unique to the GF [20,23]. For example, KGF was released from the gels *in vitro* at 5–10× the rate of Ang-1 [23]. The maturity of vessel networks elicited *in vivo* by co-delivery of VEGF+KGF from heparinized gels exceeded that elicited by VEGF+Ang-1 at both time points (VMI = 0.176 and −0.088 respectively at day 7 and 0.103 and −0.041 at day 14, Figure 6). Part of that difference in response may result simply from the difference in the rates of release of KGF and Ang-1 from the gels.

In addition, KGF was released *in vitro* from a Hp-matrix more rapidly than was VEGF [23], whereas rates of release from a non-Hp matrix may be assumed to be more comparable. Thus the ratio of primary/secondary GF, *ie* VEGF/secondary GF, present at the perimeter of the hydrogel may have been significantly different in the Hp and non-Hp cases. This ratio should affect the response in the adjacent tissue, and could explain the significantly superior VMI values attained in the Hp versus non-Hp VEGF+KGF cases (Figure 6a). Ang-1 was released *in vitro* from a Hp-matrix much less rapidly than was VEGF. The VEGF/Ang-1 ratio around the gel may explain the opposite trend found to exist between the Hp and non-Hp VEGF+Ang-1 cases.

Biologically, many fibroblast growth factors (FGFs), KGF included, require interaction with heparin to bind effectively to their associated cell surface receptors [36,37]. In fact, KGF is almost completely inactive in the absence of Hp [37]. The mitogenic effects of KGF on pericytes can therefore be expected to be strongly amplified by the presence of heparin in the gels, allowing KGF to increase maturity in elicited in-grown microvessels (Figure 8a, top). This expectation was reflected by the maturity indices at day 7 (VMI = 0.176 for HA:Hp-VEGF +KGF *vs.* −0.064 for HA-VEGF+KGF, $p < 0.012$, Figure 6a). In the non-heparinized gel, the effects of KGF were clearly attenuated at day 7, leading to decreased VMI values (Figure 8b, top). The difference in maturity response was not nearly as strong at day 14, when VMI was positive for co-delivery of VEGF and KGF in both the presence and absence of heparin in the gel. Presumably, at later times, when the gel is nearly degraded, endogenous heparin has a much stronger interaction with the delivered KGF than it does at early times.

In contrast to KGF, Ang-1 is thought to exhibit limited Hp binding capacity [38]. Consequently, the activity of exogenously delivered Ang-1 may be largely unaffected by the composition of the gel in which it is delivered. However, VEGF is activated by Hp [25,39,40], and this activation, in general, leads to both endothelial cell proliferation and pericyte regression [41]. Thus the maturity of elicited in-grown microvessels would be expected to be compromised by co-delivery of VEGF+Ang-1 from heparin-containing gels, but not by their delivery from non-heparinized gels. Both of these expectations were reflected in the VMI measurements (Figure 6a, b).

A separate mechanism by which the maturation effects of Ang-1 may be inhibited involves its indirect suppression by VEGF. Zhang *et al.* showed that Ang-2 expression in human umbilical vein endothelial cells increased significantly upon the introduction of exogenous human VEGF, and that this increase was due to VEGF-specific signal transduction rather than enhanced transcript stability [42]. In support of this, expression profiles of VEGF and Ang-2 have been found to be very tightly correlated temporally in ischemia induced angiogenesis [43]. Ang-2 competes with Ang-1 for Tie-2 binding sites [44], and when it is bound, Tie-2 signal transduction is inhibited. Inhibition of the Tie-2 signal leads to pericyte regression and decreased levels of perceived microvascular maturity [45]. The functional activity of Ang-1 may therefore be attenuated when it is co-delivered with VEGF from heparinized hydrogels, as the upregulation of VEGF activity in these hydrogels may lead to an elevation in the levels of Ang-2.

In the present experiment, the highest levels of microvessel maturity were produced by co-delivery of VEGF and PDGF from heparinized gels (VMI = −0.014 at day 7 and 0.159 at day 14, figure 6). This finding was surprising, in that PDGF-AA was previously found to be released from these gels *in vitro* at a much slower rate than either KGF or Ang-1 [23]. In addition, PDGF-AA is not known to demonstrate heparin-mediated signal transduction [46]. It seems most likely that in the presence of HA and VEGF *in vivo*, PDGF acts with much greater potency than KGF or Ang-1. Interestingly, the first FDA-approved angiogenesis-stimulating medicine in the U.S. was the wound-healing gel Regranex. It contained recombinant PDGF, and was approved in 1997 to treat diabetic foot ulcers [47].

In contrast to the HA:Hp films, the HA:Hp:Gtn-VEGF+Ang-1 and VEGF+KGF dual cytokine treatments elicited comparable levels of microvascular maturity ($p < 0.95$ at day 7 and $p < 0.90$ at day 14). The reason for this is not readily apparent. However, release rates from gelatinized and non-gelatinized matrices *in vitro* have been shown to differ significantly [23]. Interestingly, KGF is released at only 3–5× the rate of Ang-1 from a HA:Hp:Gtn matrix, a two-fold decrease from rates achieved in the non-gelatinized HA:Hp matrix.

Although HA:Hp films may effectively induce a controlled angiogenic response, in the absence of a protein component they do not support cell attachment and growth [48]. As a result, by themselves they are unsuitable for tissue regeneration. Accordingly, vascularization was also investigated for gelatin-containing gels, which have been shown to successfully foster cell attachment and growth over several weeks both *in vitro* and *in vivo* [48,49]. Almost all the HA:Hp:Gtn cases were statistically indistinguishable from the corresponding HA:Hp cases utilizing the same cytokine load. It is apparent that in general, the incorporation of Gtn into the film matrix did not adversely affect the levels of elicited microvascular maturity.

5. CONCLUSIONS

Levels of microvascular density and maturity elicited by implantation of heparinized HA-based hydrogel films pre-loaded with cytokine growth factors have been investigated *in vivo* in a mouse ear pinna model. Tissue samples retrieved at fixed times post-implantation were IHC stained for both α-SMA and vWF, and analyzed based on their staining response using separated graded indices for neovascularization (NI) and vessel maturity (VMI). It was found that the introduction of dual cytokines, one to initiate angiogenesis and the other to induce maturation, produced microvessel networks that were more mature than those produced by administration of either cytokine independently. In tissue treated with dual cytokine-loaded implants, the inclusion of heparin did not invariably lead to increased levels of microvascular maturity relative to the non-heparinized films. Instead, the inclusion of heparin had a cytokine-specific effect, promoting maturity for co-delivery of VEGF+KGF, but inhibiting maturity for delivery of VEGF+Ang-1. Characteristic Hp-mediated cytokine release rates and/or activation are thought to be responsible for these results. For nearly all treatment cases, VMI increased from day 7 to day 14 post-surgery. This provides further evidence that HA, HA:Hp and HA:Hp:Gtn films may be suitable matrices for cell encapsulation and tissue regeneration strategies. A gelation technology based on chemical modification of HA, heparin and gelatin is evidently capable of eliciting microvasculature with sustained levels of maturity, an important step in its effective application towards regenerative therapeutic strategies.

ACKNOWLEDGEMENTS

Financial support for this project was provided by Oregon State University, NIH award 1R21EB004514 and by the Utah Centers of Excellence Program. The authors wish to thank Kay Fischer and the Veterinary Medicine Diagnostic Laboratory at Oregon State University in optimizing and performing the IHC double-staining. The authors would also like to thank Dan Pike and Celeste Riley for contributing tissue blocks from previous experiments. These blocks were used in the formulation of several control cases.

REFERENCES

1. Pearson RG, Bhandari R, Quirk RA, Shakesheff KM. Recent advances in tissue engineering: an invited review. J Long Term Eff Med Implants 2002;12(1):1–33. [PubMed: 12096640]
2. Malda J, Klein TJ, Upton Z. The roles of hypoxia in the in vitro engineering of tissues. Tissue Engineering 2007;13(9):2153–2162. [PubMed: 17516855]
3. Henry TD, Abraham JA. Review of preclinical and clinical results with vascular endothelial growth factors for therapeutic angiogenesis. Curr Intervent Cardiol 2000;2:228–241.
4. Ferrara N. Vascular endothelial growth factor: molecular and biological aspects. Curr Top Microbiol Immunol 1999;237:1–30. [PubMed: 9893343]
5. Takeshita S, Zheng LP, Brogi E, Kearney M, Pu LQ, Bunting S, et al. Therapeutic angiogenesis. A single intraarterial bolus of vascular endothelial growth factor augments revascularization in a rabbit ischemic hind limb model. J Clin Invest 1994;93:662–670. [PubMed: 7509344]
6. Simons M, Bonow RO, Chronos NA, Cohen DJ, Giordano FJ, Hammond HK. Clinical trials in coronary angiogenesis: issues, problems, consensus: an expert panel summary. Circulation 2000;102:E73–E86. [PubMed: 10982554]

7. Shiu YT, Weiss JA, Hoying JB, Iwamoto MN, Joung IN. The Role of Mechanical Stresses in Angiogenesis. Critical Reviews in Biomedical Engineering 2005;33(5):431–510. [PubMed: 16000089]
8. Wang GL, Jiang BH, Rue EA, Semenza GL. Hypoxia-inducible factor 1 is a basic-helix-loop-helix-PAS heterodimer regulated by cellular O2 tension. Proc. Natl. Acad. Sci 1995;92(12):5510–5514. [PubMed: 7539918]
9. Bhattacharya R, Kang-Decker N, Hughes DA, Mukherjee P, Shah V, McNiven MA, Mukhopadhyay D. Regulatory role of dynamin-2 in VEGFR-2/KDR-mediated endothelial signaling. FASEB J 2005;19 (12):1692–1694. [PubMed: 16049137]
10. Paweletz N, Knierim M. Tumor-related Angiogenesis. Crit Rev Oncol Hematol 1989;9(3):197–242. [PubMed: 2480145]
11. Beck L, D'Amore P. Vascular development: cellular and molecular recognition. The FASEB Journal 1997;11:365–373. [PubMed: 9141503]
12. Davis G, Senger D. Endothelial Extracellular Matrix: Biosynthesis, Remodeling, and Functions During Vascular Morphogenesis and Neovessel Stabilization. Circulation Research 2005;97:1093–1107. [PubMed: 16306453]
13. Reinmuth N, Stoeltzing O, Liu W, Ahmad SA, Jung YD, Fan F, Parikh A, Ellis LM. Endothelial survival factors as targets for antineoplastic therapy. Cancer J 2001:S109–S119. [PubMed: 11779081]
14. Yonenaga Y, Mori A, Onodera H, Yasuda S, Oe H, Fujimoto A, Tachibana T, Imamura M. Absence of smooth muscle actin-positive pericyte coverage of tumor vessels correlates with hematogenous metastasis and prognosis of colorectal cancer patients. Oncology 2005;69(2):159–166. [PubMed: 16127287]
15. Taylor A, Rodriguez M, Adams K, Goldenberg D, Blumenthal R. Altered Tumor Vessel Maturation and Proliferation in Placenta Growth Factor –Producing Tumors: Potential Relationship to Post-Therapy Tumor Angiogenesis and Recurrence. Int. J. Cancer 2003;105:158–164. [PubMed: 12673673]
16. Bartels U, Hawkins C, Jing M, Ho M, Dirks P, Rutka J, Stephens D, Bouffet E. Vascularity and angiogenesis as predictors of growth in optic pathway/hypothalamic gliomas. J Neurosurg 2006;104:314–320. [PubMed: 16848088]
17. Riley CM, Fuegy PW, Firpo MA, Shu XZ, Prestwich GD, Peattie RA. Stimulation of in vivo angiogenesis using dual growth factor-loaded crosslinked glycosaminoglycan hydrogels. Biomaterials 2006;27(35):5935–5943. [PubMed: 16950508]
18. Peattie RA, Rieke ER, Hewett EM, Fisher RJ, Shu XZ, Prestwich GD. Dual growth factor-induced angiogenesis in vivo using hyaluronan hydrogel implants. Biomaterials 2006;27(9):1868–1875. [PubMed: 16246413]
19. Peattie RA, Nayate AP, Firpo MA, Shelby J, Fisher RJ, Prestwich GD. Stimulation of in vivo angiogenesis by cytokine-loaded hyaluronic acid hydrogel implants. Biomaterials 2004;25:2789–2798. [PubMed: 14962557]
20. Pike DB, Cai S, Pomraning KR, Firpo MA, Fisher RJ, Shu XZ, Prestwich GD, Peattie RA. Heparin-regulated release of growth factors in vitro and angiogenic response in vivo to implanted hyaluronan hydrogels containing VEGF and bFGF. Biomaterials 2006;27(30):5242–5251. [PubMed: 16806456]
21. Prestwich GD. Simplifying the Extracellular Matrix for 3-D Cell Culture and Tissue Engineering: A Pragmatic Approach. J Cell Biochem 2007;101:1370–1383. [PubMed: 17492655]
22. Slevin M, Krupinski J, Gaffney J, Matou S, West D, Delisser H, Savani RC, Kumar S. Hyaluronan-mediated angiogenesis in vascular disease: uncovering RHAMM and CD44 receptor signaling pathways. Matrix Biol 2007;26(1):58–68. [PubMed: 17055233]
23. Peattie RA, Yu B, Cai S, Pike D, Firpo MA, Fisher RJ, Shu XZ, Prestwich GD. Heparin Regulation of Cytokine Release from Hyaluronan-based Hydrogels *In Vitro*. In review: J Biomed Mat Res. 2006
24. Cai S, Liu Y, Zheng Shu X, Prestwich GD. Injectable glycosaminoglycan hydrogels for controlled release of human basic fibroblast growth factor. Biomaterials 2005;26(30):6054–6067. [PubMed: 15958243]

25. Robinson JR, Mulloy B, Gallagher JT, Stringer SE. $VEGF_{165}$-binding Sites within Heparan Sulfate Encompass Two Highly Sulfated Domains and Can Be Liberated by K5 Lyase. J Biol Chem 2006;281 (3):1731–1740. [PubMed: 16258170]
26. Thompson LD, Pantoliano MW, Springer BA. Energetic Characterization of the basic fibroblast growth factor-heparin interaction: identification of the heparin binding domain. Biochemistry 1994;33(13):3831–3840. [PubMed: 8142385]
27. Onda M, Naito Z, Wang R, Fujii T, Kawahara K, Ishiwata T, Sugisaki Y. Expression of keratinocyte growth factor receptor (KGFR/KGFR2 IIIb) in vascular smooth muscle cells. Pathol Int 2003;53(2): 127–132. [PubMed: 12608893]
28. D'Amore PA, Smith SR. Growth factor effects on cells of the vascular wall: a survey. Growth Factors 1993;8(1):61–75. [PubMed: 7680568]
29. Shu XZ, Liu Y, Luo Y, Roberts M, Prestwich GD. Disulfide Cross-Linked Hyaluronan Hydrogels. Biomacromolecules 2002;3:1304–1311. [PubMed: 12425669]
30. Butterworth P, Baum H, Porter J. A modification of the Ellman procedure for the estimation of protein sulfhydryl groups. Arch Biochem Biophys 1967;118:716–723. [PubMed: 6069104]
31. Shu XZ, Liu Y, Palumbo FS, Luo Y, Prestwich GD. In situ crosslinkable hyaluronan hydrogels for tissue engineering. Biomaterials 2004;25:1339–1348. [PubMed: 14643608]
32. Hosack, LW. Thesis. Oregon State U; 2007. Determining cytokine induced vascular maturity through immunohistochemical double-staining. Available online: http://hdl.handle.net/1957/5992
33. Liu Y, Cai S, Shu XZ, Shelby J, Prestwich GD. Release of basic fibroblast growth factor from crosslinked glycosaminoglycan hydrogel promotes wound healing. Wound Repair Regen 2007;15 (2):245–251. [PubMed: 17352757]
34. Gerhardt H, Golding M, Fruttiger M, Ruhrberg C, Lundkvist A, Abramsson A, Jeltsch M, Mitchell C, Alitalo K, Shima D, Betsholtz C. VEGF guides angiogenic sprouting utilizing endothelial tip cell filopedia. J Cell Biol 2003;161(6):1163–1177. [PubMed: 12810700]
35. Armulik A, Abramsson A, Betsholtz C. Endothelial/pericyte interactions. Circ Res 2005;97(6):512–523. [PubMed: 16166562]
36. Lodish, H.; Baltimore, D.; Berk, A.; Zipursky, S.; Matsudaira, P.; Darnell, J. Molecular Cell Biology. 3rd edition. New York: Scientific American Books, Inc.; 1995.
37. Berman B, Ostrovsky O, Shlissel M, Lang T, Regan D, Vlodavsky I, Ishai-Michaeli R, Ron D. Similarities and Differences between the Effects of Heparin Glypican-1 on the Bioactivity of Acid Fibroblast Growth Factor and the Keratinocyte Growth Factor. The Journal of Biological Chemistry 1999;274(51):36132–36138. [PubMed: 10593896]
38. Yin X, Qin Y. Angiopoietin-1, Unlike Angiopoietin-2, Is Incorporated into the Extracellular Matrix via Its Linker Peptide Region. The Journal of Biological Chemistry 2001;276(37):34990–34998. [PubMed: 11447223]
39. Gitay-Goren H, Soker S, Vlodavsky I, Neufeld G. The binding of vascular endothelial growth factor to its receptors is dependent on cell surface-associated heparin-like molecules. J Biol Chem 1992;267 (9):6093–6098. [PubMed: 1556117]
40. Ashikari-Hada S, Habuchi H, Kariya Y, Kimata K. Heparin Regulates Vascular Endothelial Growth $Factor_{165}$-dependent Mitogenic Activity, Tube Formation, and Its Receptor Phosphorylation of Human Endothelial Cells: Comparison of the Effects of Heparin and Modified Heparins. The Journal of Biological Chemistry 2005;280(36):31508–31515. [PubMed: 16027124]
41. Darland D, D'Amore P. Blood vessel maturation: vascular development comes of age. JCI 1999;103 (2):157–158. [PubMed: 9916126]
42. Zhang L, Yang N, Park J, Katsaros D, Fracchioli S, Cao G, Jenkins A, Randall T, Rubin S, Coukos G. Tumor-derived Vascular Endothelial Growth Factor Up-Regulates Angiopoietin-2 in Host Endothelium and Destabilizes Host Vasculature, Supporting Angiogenesis in Ovarian Cancer. Cancer Research 2003;63:3403–3412. [PubMed: 12810677]
43. Matsunaga T, Warltier D, Tessmer J, Weihrauch D, Simons M, Chilian W. Expression of VEGF and angiopoietins-1 and 2 during ischemia-induced coronary angiogenesis. Am J Physiol Heart Circ Physiol 2003;285:H352–H358. [PubMed: 12649074]
44. Christensen RA, Fujikawa K, Madore R, Oettgen P, Varticovski L. NERF2, a member of the Ets family of transcription factors, is increased in response to hypoxia and angiopoietin-1: a potential

mechanism for Tie2 regulation during hypoxia. J Cell Biochem 2002;85(3):505–515. [PubMed: 11967990]

45. Cao Y, Sonveaux P, Liu S, Zhao Y, Clary BM, Li CY, Kontos CD, Dewhirst MW. Systemic overexpression of angiopoietin-2 promotes tumor microvessel regression and inhibits angiogenesis and tumor growth. Cancer Res 2007;67(8):3835–3844. [PubMed: 17440098]
46. Rolny C, Spillman D, Lindahl U, Claesson-Welsh L. Heparin Amplifies Platelet-derived Growth Factor (PDGF)-BB induced PDGF α-Receptor but not PDGF β-Receptor Tyrosine Phosphorylation in Heparin Sulfate-deficient Cells: Effects on Signal Transduction and Biological Responses. The Journal of Biological Chemistry 2002;277(22):19315–19321. [PubMed: 11912193]
47. Davis ME, Hsieh PCH, Grodzinsky AJ, Lee RT. Custom Design of the Cardiac Microenvironment with Biomaterials. Circ. Res 2005;97:8–15. [PubMed: 16002755]
48. Shu XZ, Liu Y, Palumbo F, Prestwich GD. Disulfide-crosslinked hyaluronan-gelatin hydrogel films: a covalent mimic of the extracellular matrix for in vitro cell growth. Biomaterials 2003;24(21):3825–3834. [PubMed: 12818555]
49. Shu XZ, Ahmad S, Liu Y, Prestwich GD. Synthesis and evaluation of injectable, in situ crosslinkable synthetic extracellular matrices for tissue engineering. J Biomed Mater Res A 2006;79(4):902–912. [PubMed: 16941590]

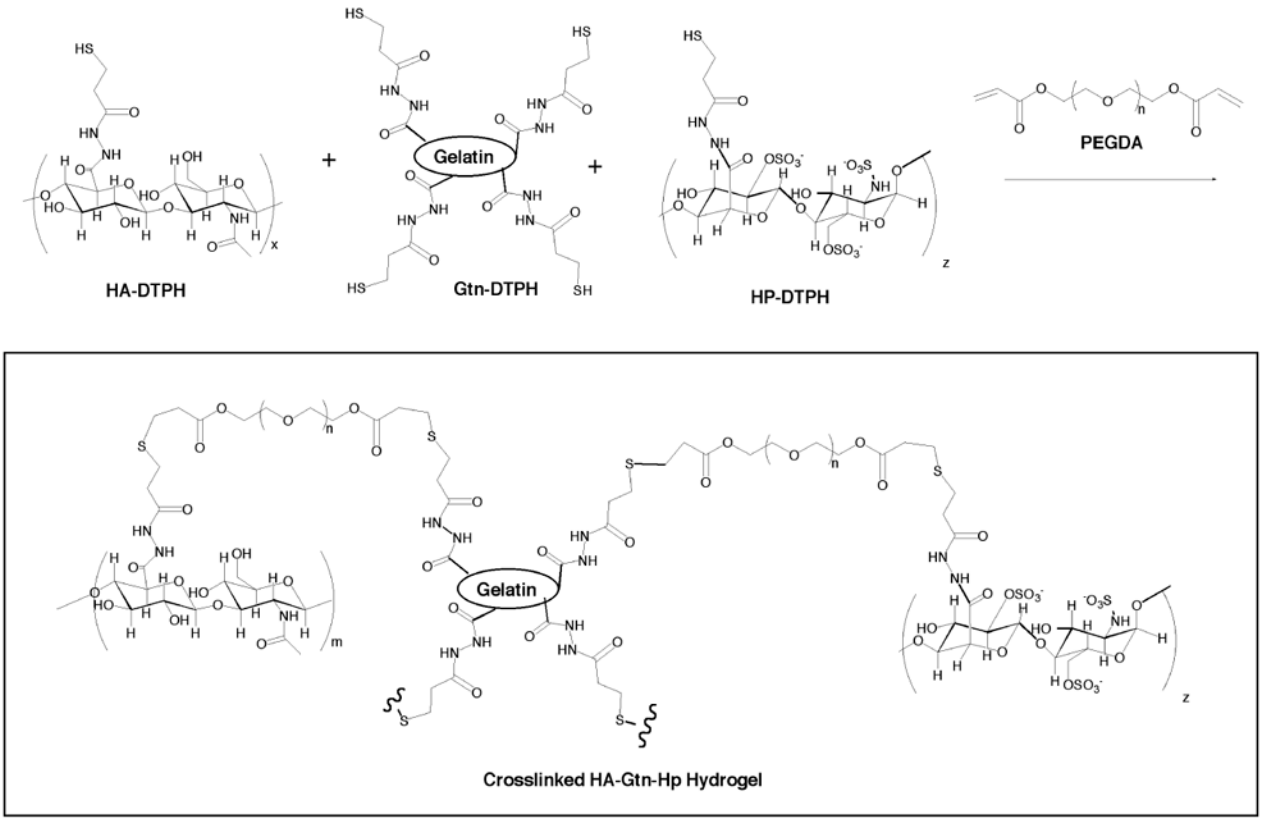

Figure 1.
Chemical structure of crosslinked HA-DTPH, Hp-DTPH and Gtn-DTPH.

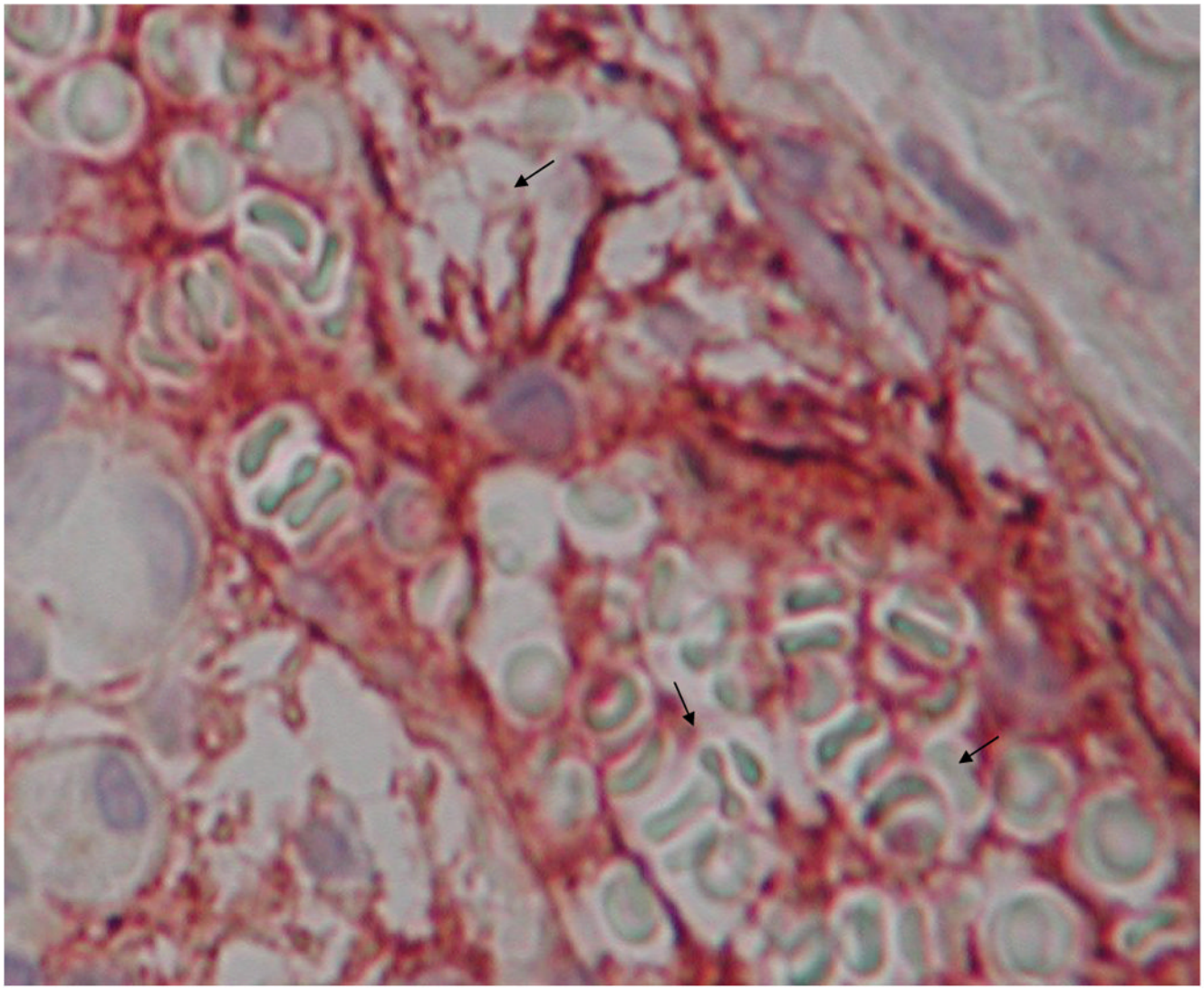

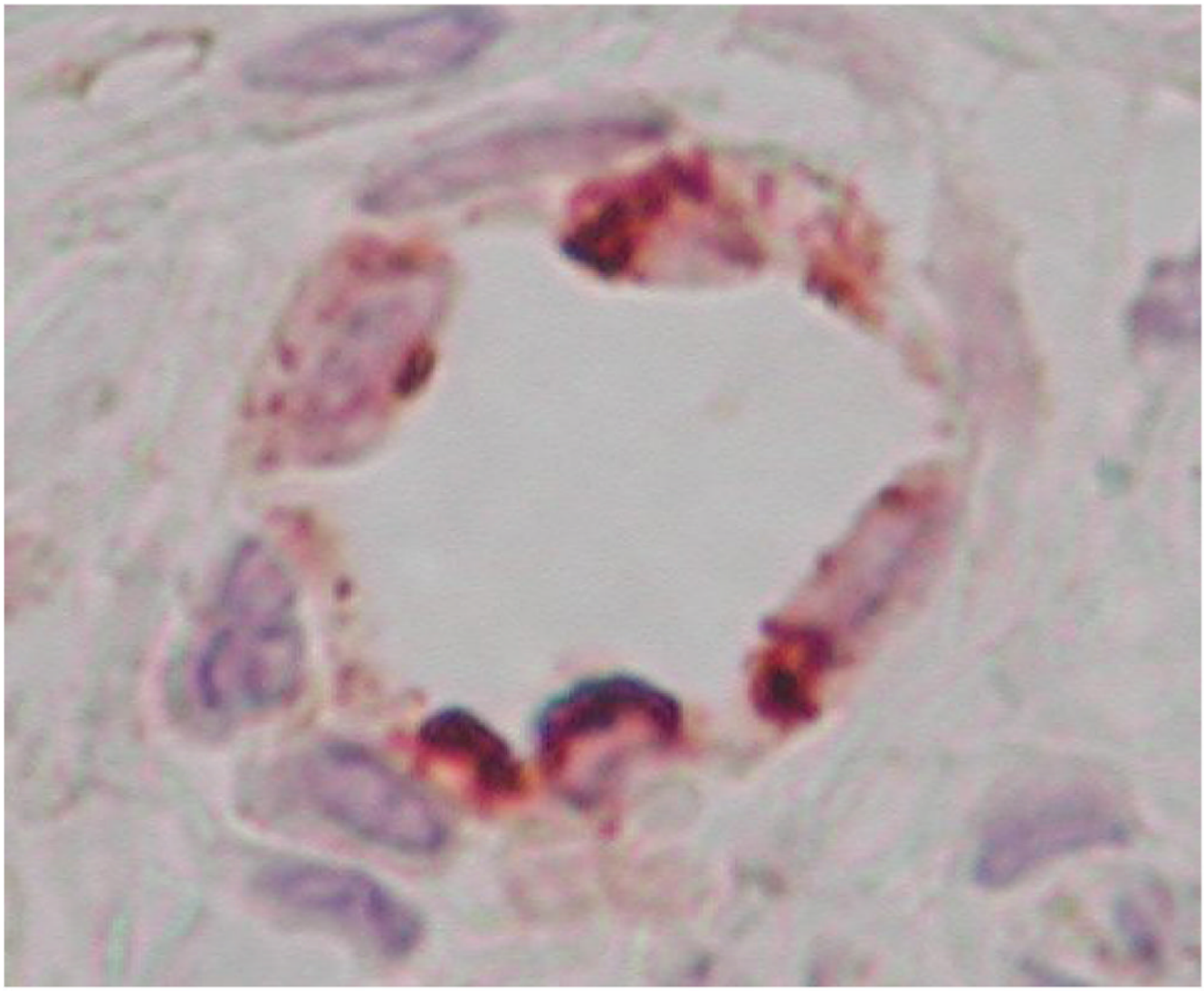

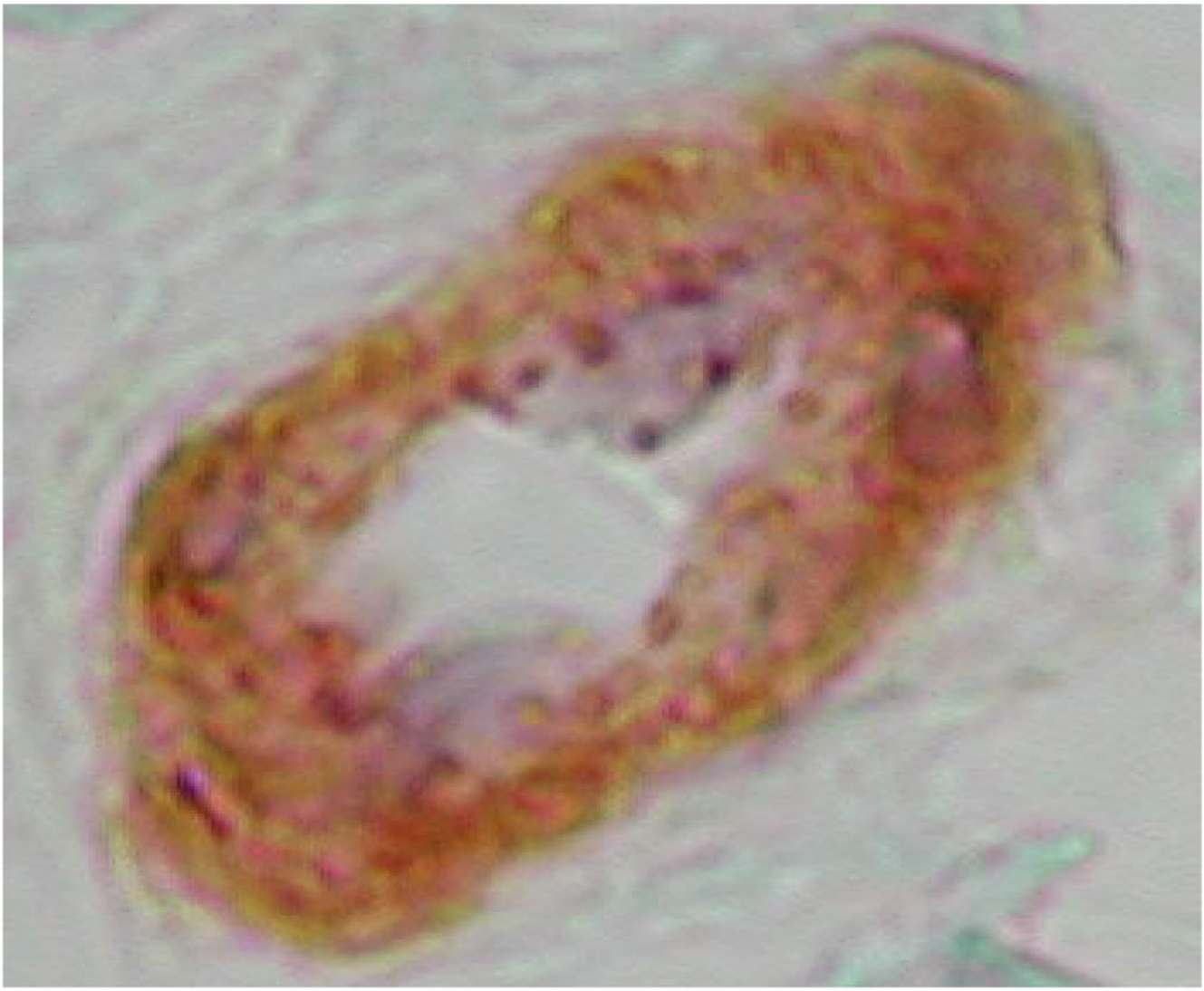

Figure 2.
Microvasculature representative of the three bins used to categorize levels of maturity, IHC double stained for α-SMA (brown) and vWF (red). Bin 1 microvasculature (a) often exhibited a primitive honeycombed appearance with extensive hyperfusion (arrows), and an absence of clearly defined endothelial borders. Bin 2 microvessels (b) were distinguishable from bin 1 vessels primarily by the existence of clearly defined borders. Some of the bin 2 microvessels displayed α-SMA signal over less than 1/3 of the total perimeter. Bin 3 microvessels (c) exhibited both clearly defined endothelial borders and extensive α-SMA signal. Bin 3 microvessels were completely circumscribed by pericytes.

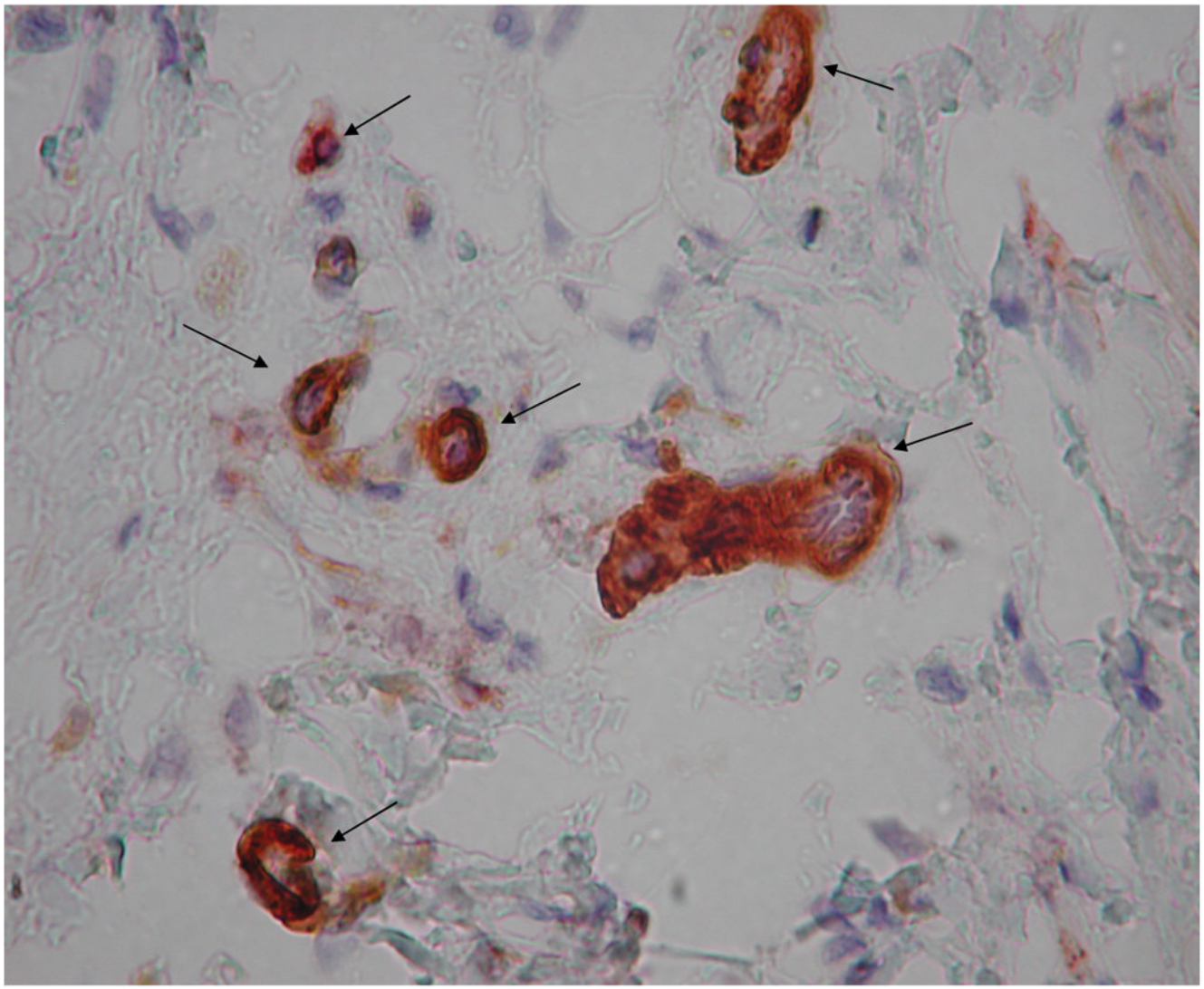

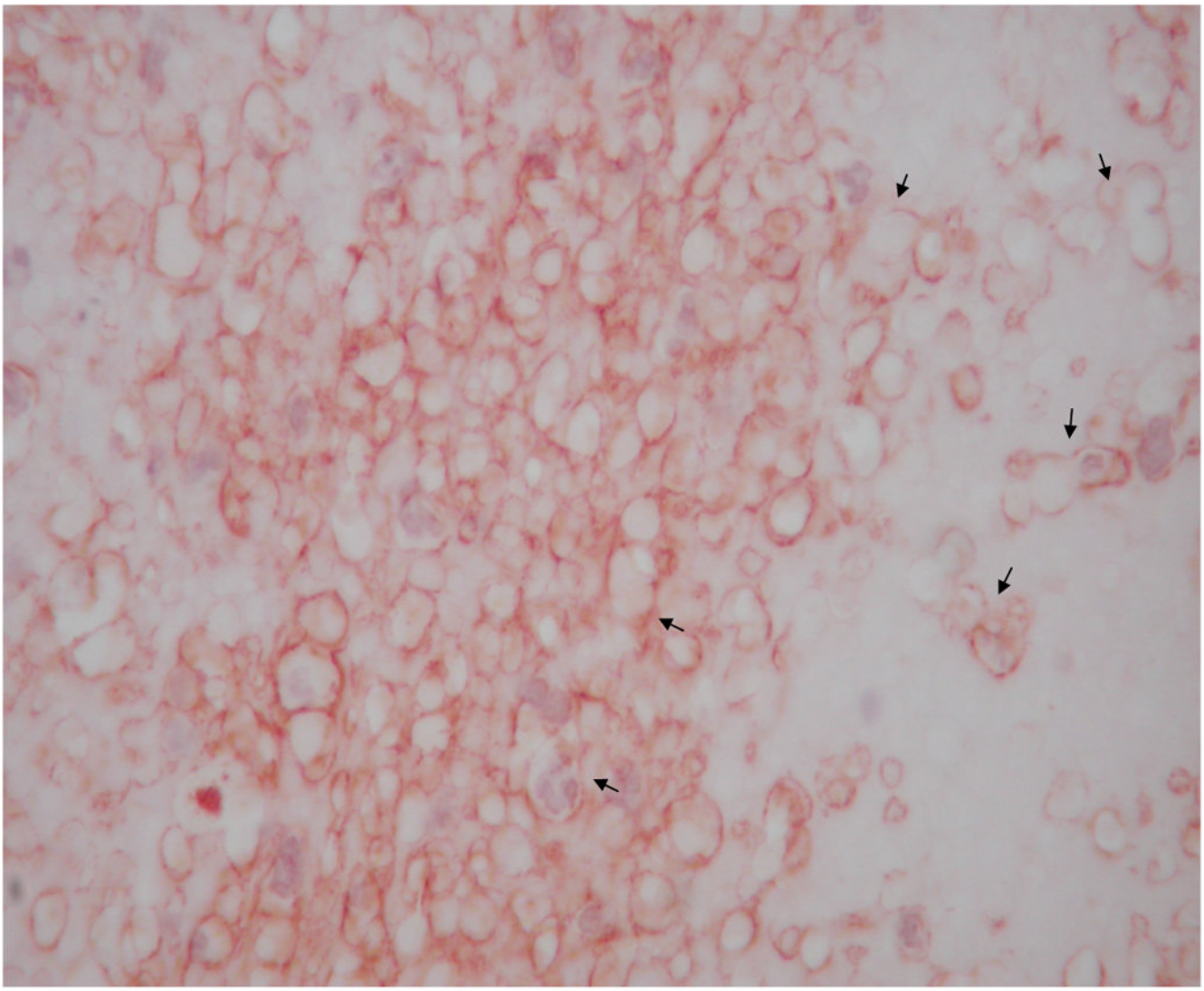

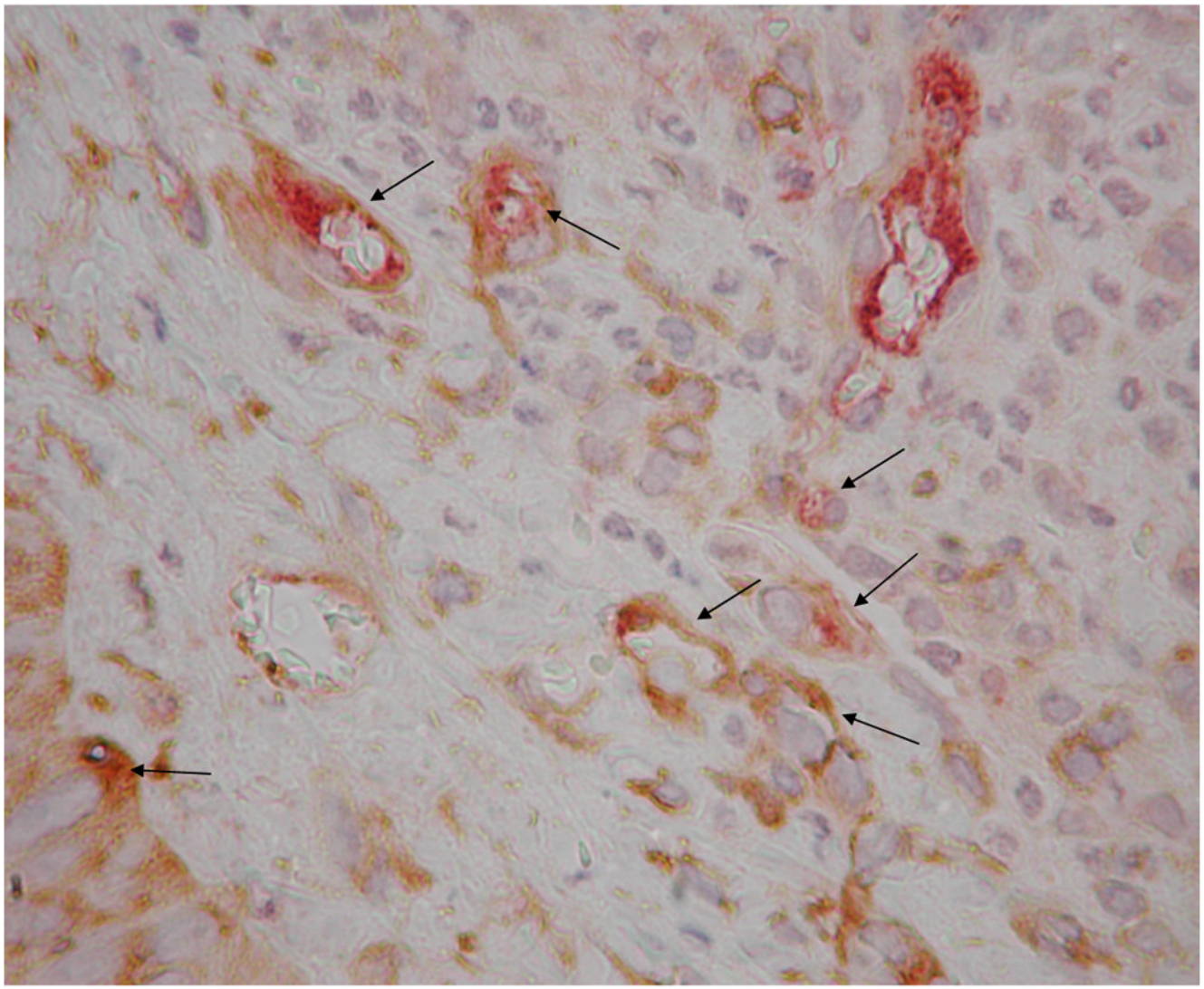

Figure 3.

Representative images of microvasculature at 7 days post-surgery, IHC double stained for α-SMA (brown) and vWF (red), 400×. The contralateral ear (a) exhibited mature vasculature (bin 3 microvessels indicated by long arrows). There were no hyperfused capillary networks in these ears and, in general, vascular densities were relatively low. Time related variations in vasculature were minimal to non-existent. HA:Hp-VEGF treated tissue exhibited the least mature vasculature at 7 days post surgery (b). All hyperfused vessels in this field (short arrows) were characterized as bin 1, due to the lack of both clearly defined endothelial borders as well as pericyte association. HA:Hp-VEGF+KGF treated tissue (c) exhibited, by far, the most mature vasculature of all 7 day experimental cases (all vessels belonging to bin 3 are indicated by long arrows).

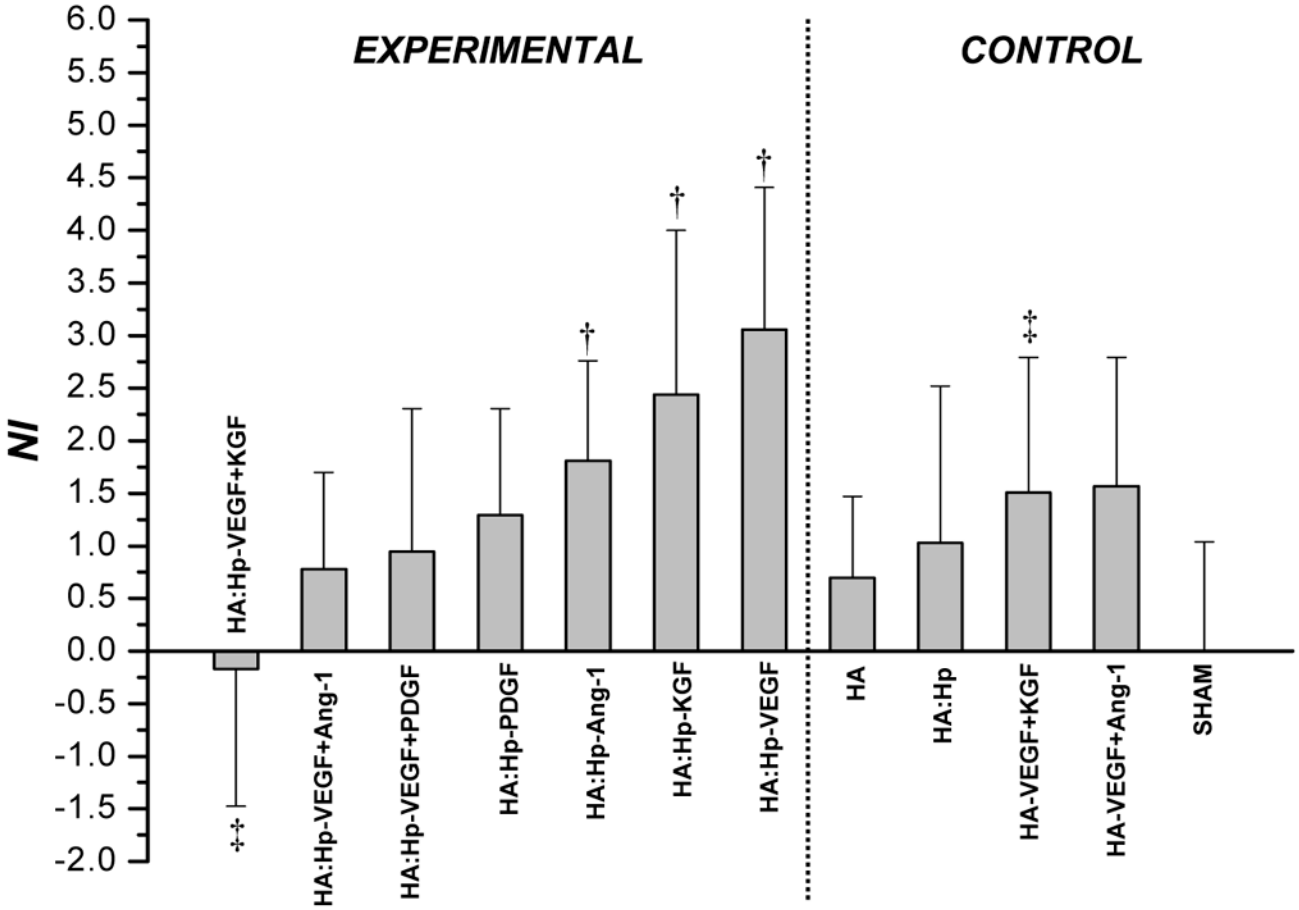

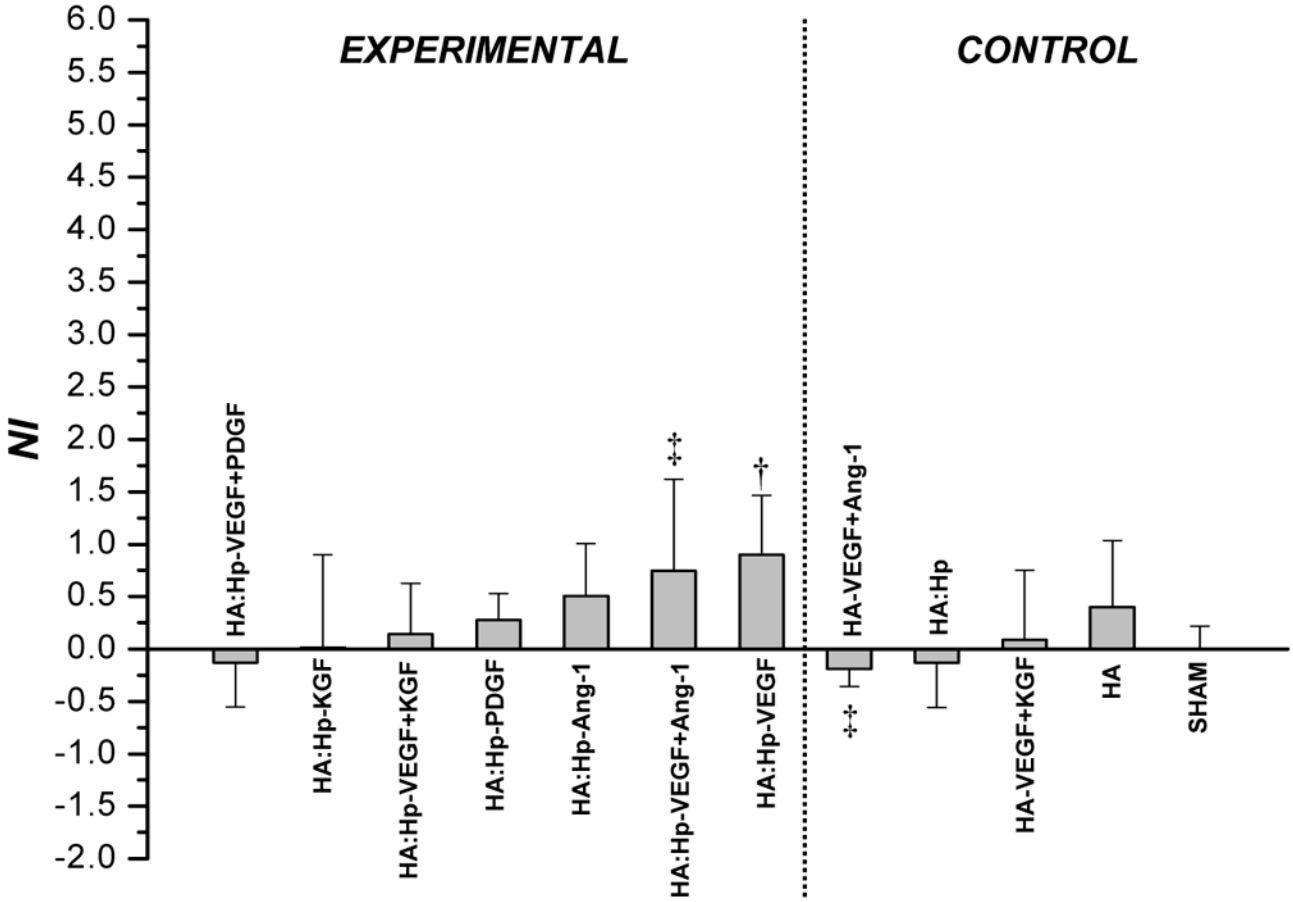

Figure 4.

NI values attained from tissue treated with HA:Hp cytokine loaded experimental gels at 7 days (a) and 14 days (b) post-implantation. NI is defined in text, Eq. (1). Mean ± s.d., n=3; † $p < 0.05$ vs. sham control; ‡ $p \leq 0.05$ for pairwise comparison between experimental (HA:Hp) and control (HA) treatments utilizing the same cytokine combination.

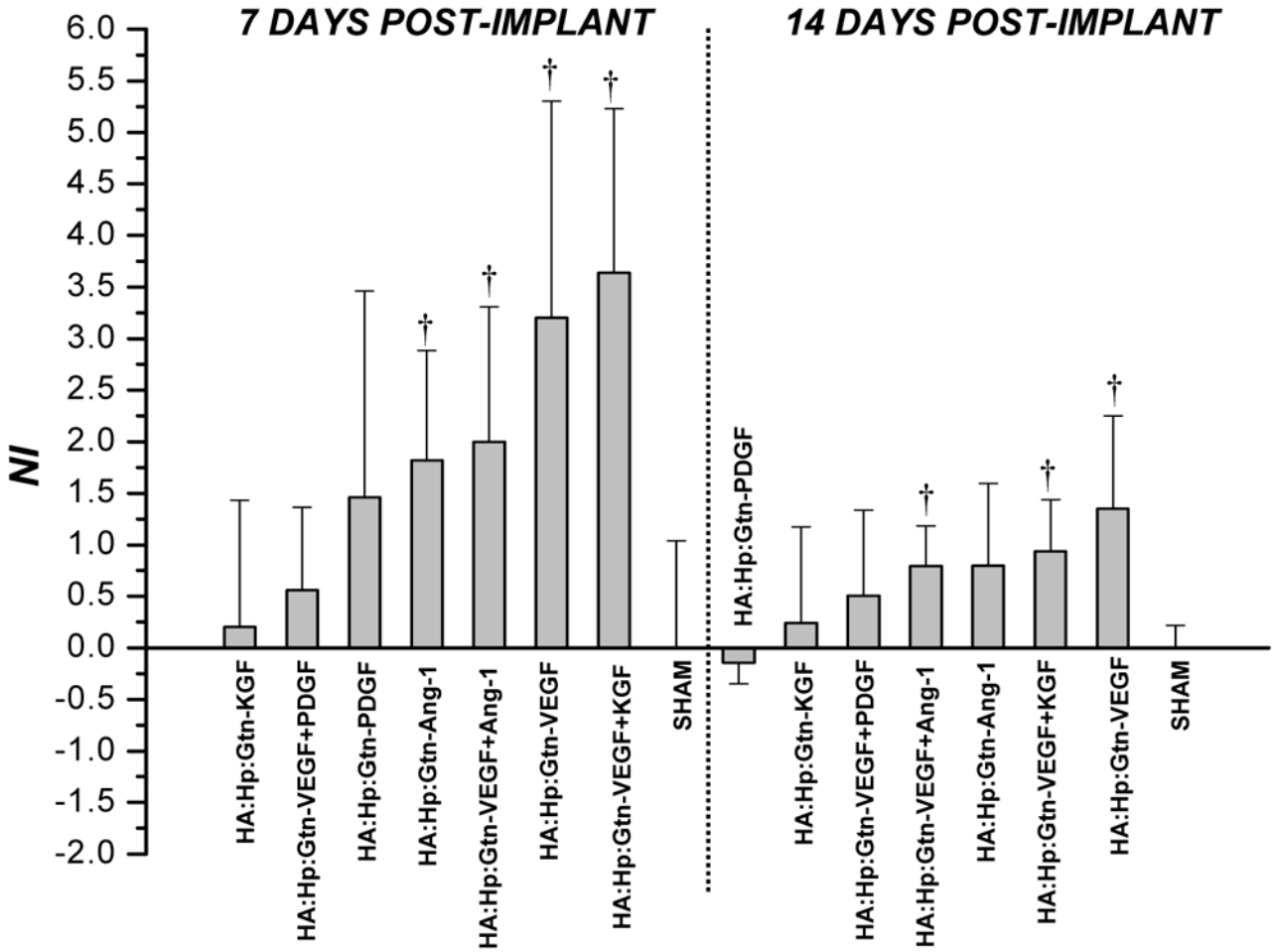

Figure 5.
NI values attained from tissue treated with HA:Hp:Gtn cytokine loaded experimental gels at 7 and 14 days post-implantation. NI is defined in text, Eq. (1). Mean ± s.d., n=3; † $p < 0.05$ vs. sham control.

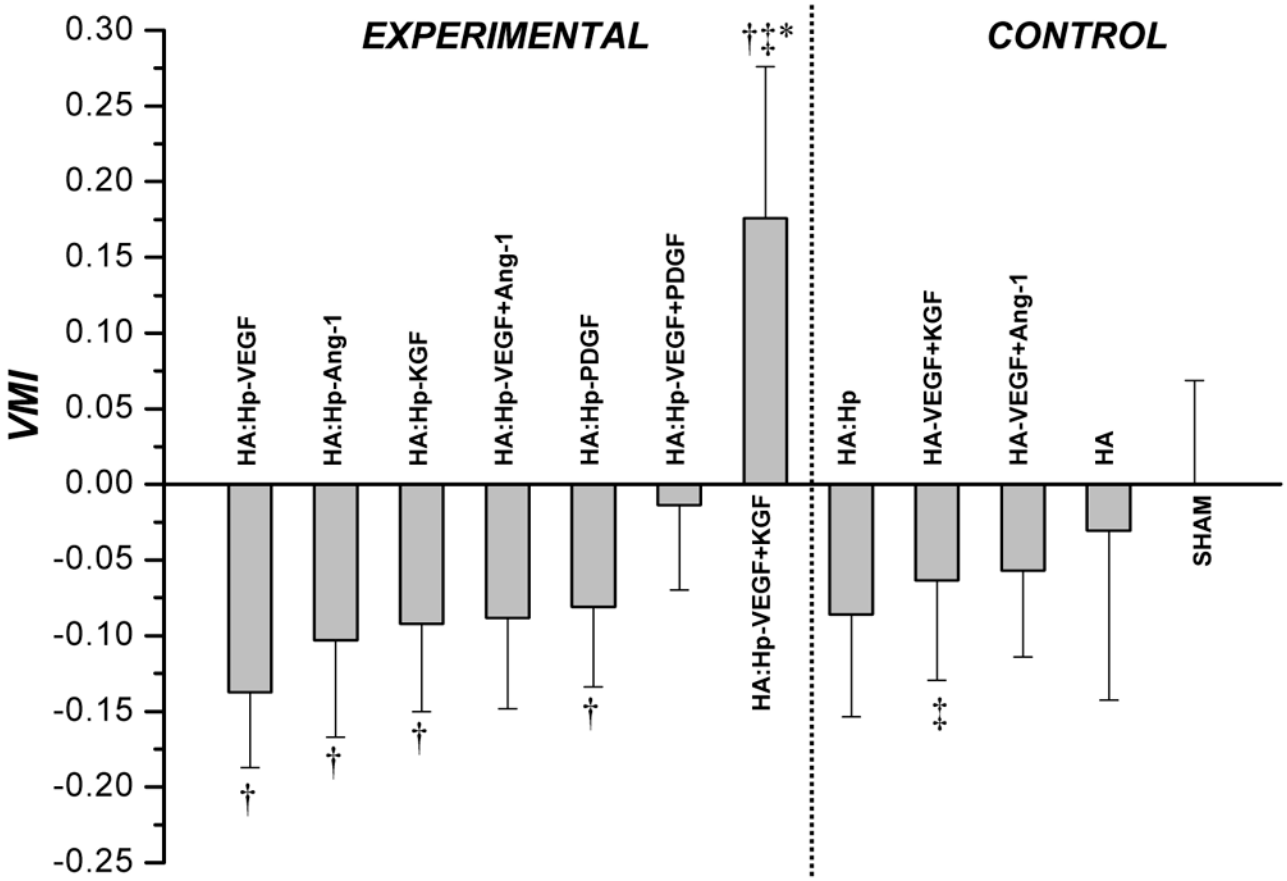

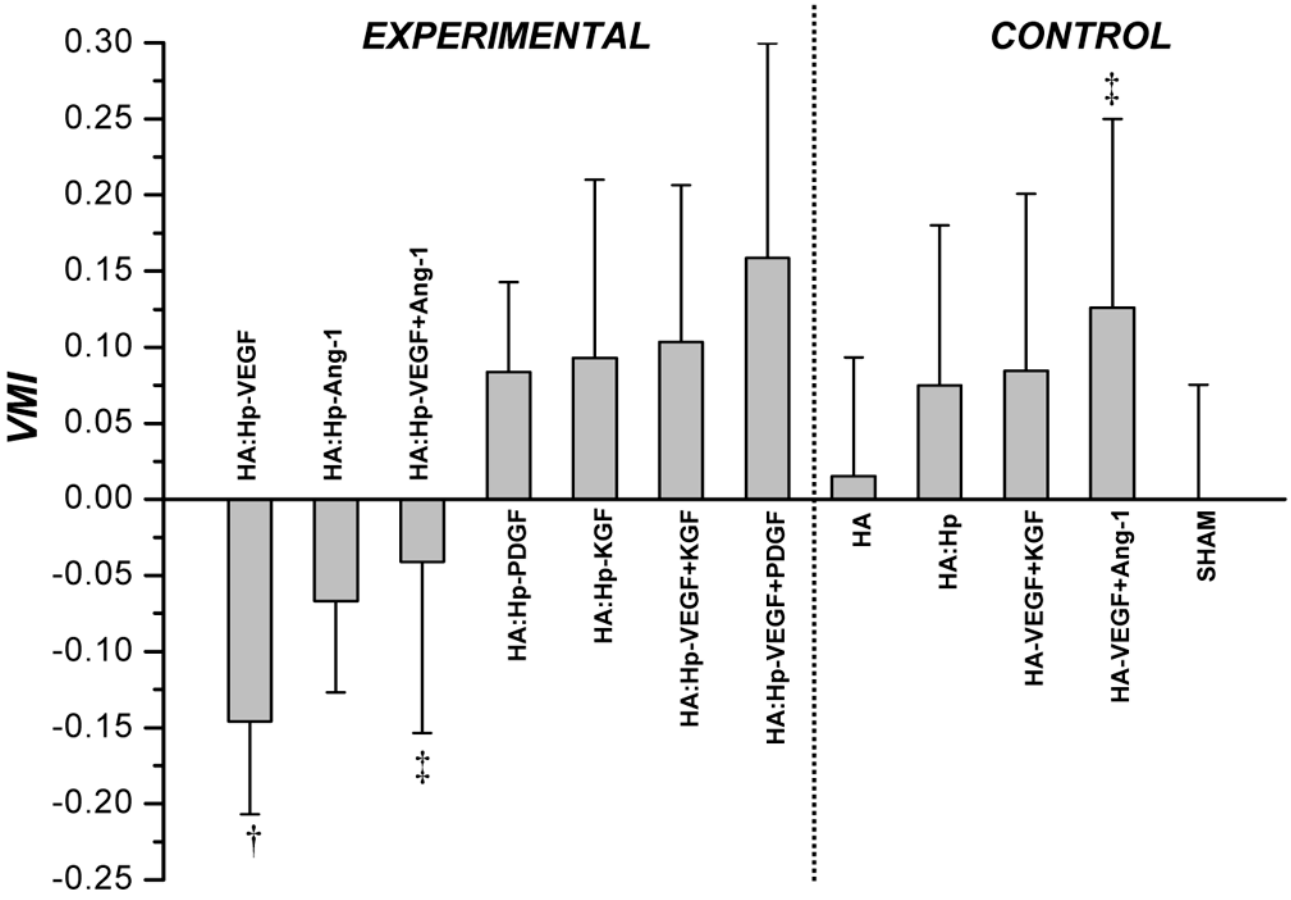

Figure 6.

VMI values attained from tissue treated with control and cytokine loaded HA:Hp films at 7 days (a) and 14 days (b) post surgical implantation. VMI is defined in the text, Eq. (2). Mean ± s.d., n = 3; *$p \leq 0.05$ vs. all other treatment cases; † $p \leq 0.05$ vs. sham control; ‡ $p \leq 0.05$ for pairwise comparison between experimental (HA:Hp) and control (HA) treatments utilizing the same cytokine combination.

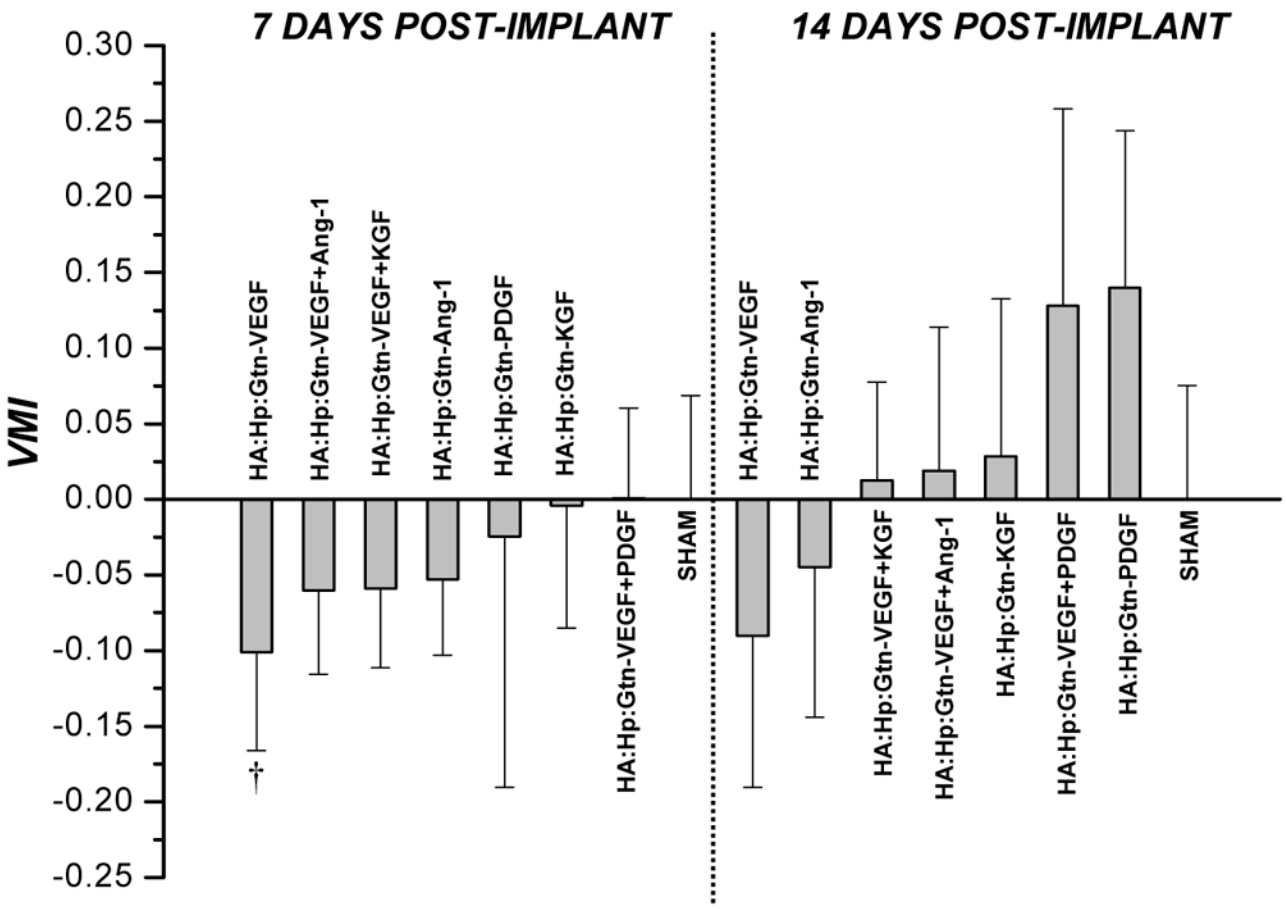

Figure 7.

VMI values attained from tissue treated with cytokine loaded HA:Hp:Gtn gels at 7 and 14 days post surgical implantation. VMI is defined in the text, Eq. (2). Mean ± s.d., n = 3; † $p \leq 0.05$ vs. sham control.

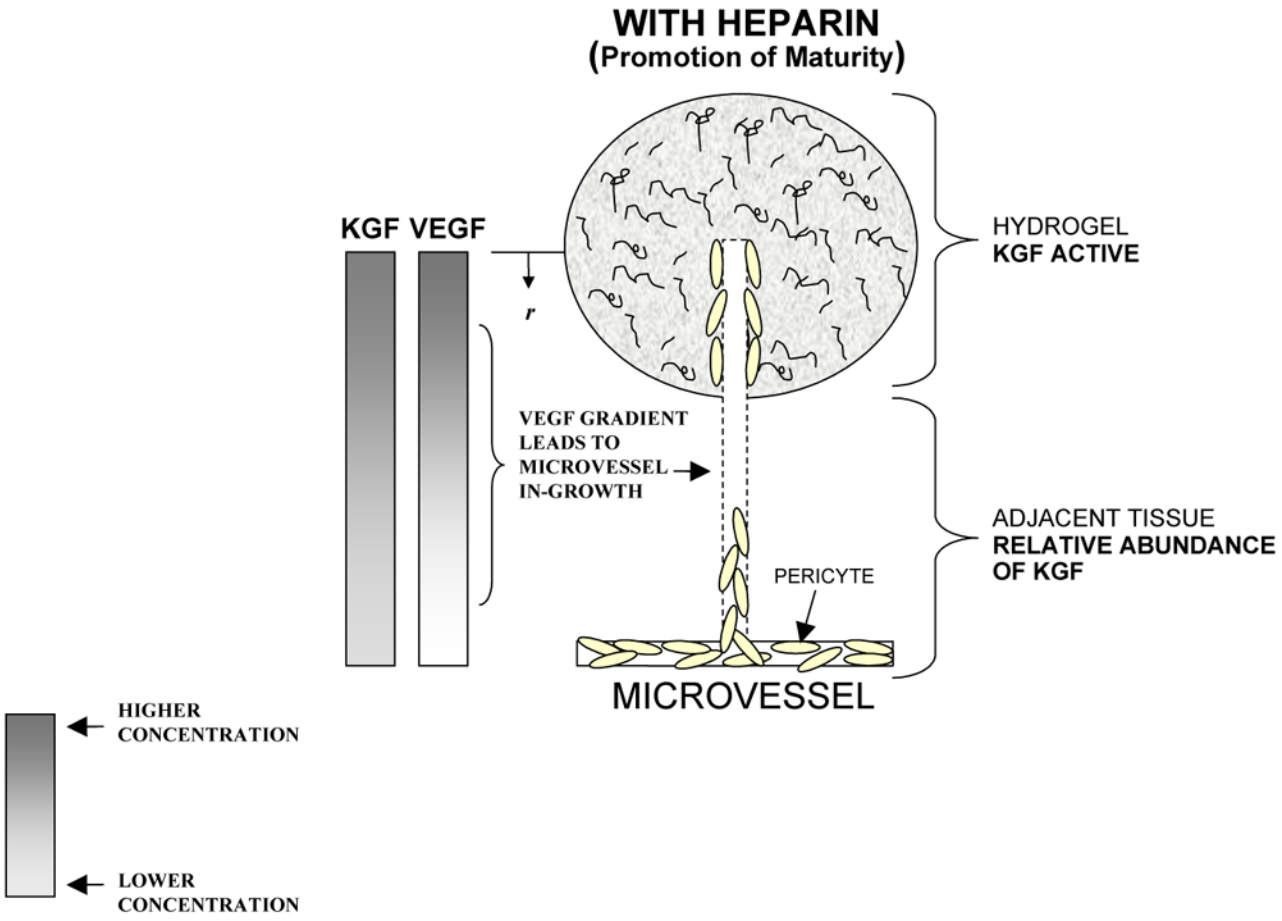

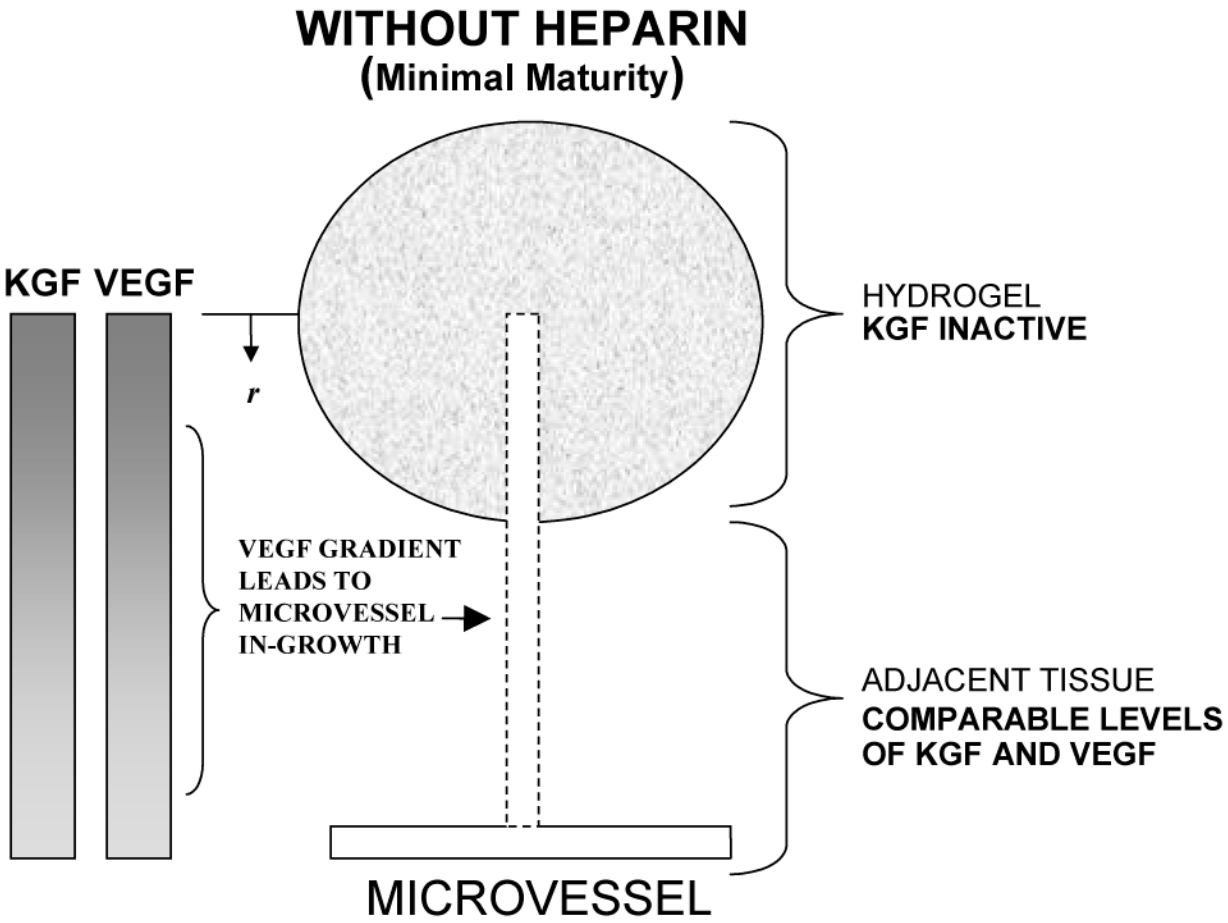

Figure 8.

Schematic depiction of microvascular growth and maturation in tissue treated with heparinized and non-heparinized VEGF+KGF loaded hydrogels. In tissue treated with heparinized VEGF +KGF hydrogels (a), elevated levels of microvascular maturity may occur in VEGF induced in-growth due to Hp-mediated KGF activation (top). In addition, elevated levels of maturity may also exist in the adjacent tissue, and this response may be characterized by a relative abundance of KGF (bottom). KGF exists in higher concentrations than does VEGF due to its characteristically rapid release from Hp-matrix, as visualized by the representative concentration gradients for VEGF and KGF, at left. In tissue treated with non-heparinized VEGF+KGF hydrogels (b), decreased VMI values occur by virtue of KGF inactivity (top), and/or comparable VEGF and KGF matrix release (bottom).